Thin Solid Films xxx (2009) xxx–xxx

Contents lists available at ScienceDirect

Thin Solid Films

journal homepage: www.elsevier.com/locate/tsf

Effect of laser flux density on ZnCdS thin films

Sonal Singhal [a,b], Amit Kumar Chawla [a], Hari Om Gupta [b], Ramesh Chandra [a,*]

[a] Nanoscience Laboratory, Institute Instrumentation Center, Indian Institute of Technology Roorkee, Roorkee – 247667, India
[b] Department of Electrical Engineering, Indian Institute of Technology Roorkee, Roorkee – 247667, India

ARTICLE INFO

Available online xxxx

Keywords:
Nanophosphor
XRD
AFM
Laser flux density

ABSTRACT

Effect of laser flux density on the structural quality and optical properties of $Zn_{0.6}Cd_{0.4}S$ thin films synthesized by ultraviolet pulsed laser deposition have been studied. The stoichiometric composition of this alloy was estimated using lattice constant calculated via XRD data. Surface morphology of the samples was examined using AFM. Optical properties were studied at room temperature by transmittance, absorbance, and photoluminescence measurements. Studies revealed that there is an improvement in the structural quality with increasing the laser flux density in some range. However, too high laser flux density could lead to the degradation in structural quality of thin film. It was observed from the PL data that with increase in laser flux density there is a decrease in the band gap. Transmission data shows a transmittance of more than 70% in the visible region. TEM investigation of the samples reveals that the particles are spherical in shape with average diameter of 15 nm.

1. Introduction

II–VI Zn based ternaries are mostly important in the production of devices such as short wavelength emitting laser diodes and light emitting diodes. When they are deposited as thin films, these alloys give the possibility of tailoring devices showing band gap engineering [1–3]. Furthermore, their electronic band structure and wide range of band gap together with a low refractive index allow intense light transmission and also effective electron transport at high electric field. The interest in Zn based ternaries is also particularly concerned with increasing demand for materials useful for the production of flat panel display, high efficiency electroluminescent and field emission devices [1,2]. Nevertheless, they show a lower crystallinity, with respect to other semiconducting compounds; therefore they are highly defective and their structural properties are mainly linked to the growth processes used for the layer deposition [4,5]. Among the new and up to date techniques used for thin film deposition, pulsed laser deposition (PLD) is one of the most versatile methods to obtain layers of several materials that can be processed into a pellet target. One of the important features of this method is based on the possibility of maintaining the stoichiometry of the ablated target in the deposited layer [6–8]. The target ablated by laser can create a highly energetic growth precursor, leading to non equilibrium growth conditions. Therefore high quality films can be obtained at a fairly low substrate temperature. Furthermore, PLD is more flexible than other conventional techniques, and it is feasible to control the thickness of films [9,10]. With this aim, in the current work, we study the influence of the laser flux density on the crystalline quality, the surface morphology, and the optical properties of the $Zn_{1-x}Cd_xS$ thin films on glass substrate grown by pulsed laser deposition.

2. Experimental

In the present work $Zn_{0.6}Cd_{0.4}S$ films with varying laser fluence were deposited on corning 1737 glass substrates by ablating stoichiometric home-made targets using pulse laser deposition technique. Targets for laser ablation were obtained by applying uniaxial pressure (18–20 t) on the $Zn_{1-x}Cd_xS$ powders prepared by a co-precipitation method. Value of x in the target material has been controlled by taking appropriate molar amount of salts containing Cadmium and Zinc. We have used 0.5 M of Zinc Nitrate and 0.2 M of Cadmium nitrate to obtain the mole fraction (x) as 0.4. Depositions were carried out with a KrF excimer laser (Lambda Physik) operating at 248 nm. Substrate and target were placed in a custom designed vacuum chamber (Excel Instruments) and was maintained at base vacuum of 5×10^{-6} torr with the aid of rotary and turbo molecular pump. The distance between the target and the substrate was maintained at 30 mm. The target was rotated at 20 rpm to preclude pit formation on the target surface and to ensure uniform ablation of the target. Pulsed laser used for ablation was set with a pulse width of 25 ns and with a repetition rate of 10 Hz. During the film deposition the substrate temperature and ambient pressure were kept at 400 °C and 10^{-5} torr respectively. In order to investigate the effect of laser flux density on the structural and optical properties of $Zn_{1-x}Cd_xS$ thin film, a series of samples with mole fraction "$x=0.4$" were deposited using the laser flux density of 2.5 J/cm^2, 3.33 J/cm^2 and 4.16 J/cm^2.

* Corresponding author. Tel.: +91 1332 285743; fax: +91 1332 286303.
E-mail address: ramesfic@iitr.ernet.in (R. Chandra).

0040-6090/$ – see front matter © 2009 Elsevier B.V. All rights reserved.
doi:10.1016/j.tsf.2009.09.115

Table 1
Sample roughness, average particle sizes calculated from the Scherrer equation and observed from AFM, emission wavelength, refractive index and band gap with varying laser flux density.

Sample	Laser flux density (J/cm^2)	Roughness (rms) (nm)	d_{XRD} (nm)	Emission wavelength (nm)	Refractive index	Band gap (eV)
Sample-1	2.5	11.3	13.2	424	1.95	2.95
Sample-2	3.33	4.8	15.5	425	1.92	2.94
Sample-3	4.16	20.1	17.3	429	1.89	2.90

X-ray diffraction (XRD) analysis was performed by using a Bruker D8 Advance diffractometer using CuK_α ($\lambda = 1.54$ Å) radiation. Surface morphology of the deposited films was studied using NT-MDT Ntegra atomic force microscopy (AFM). Room temperature transmittance and absorbance spectra were measured in the spectral range from 200 to 800 nm using a Ultra violet–Visible–Near infrared (UV–Vis–NIR) spectrophotometer (Varian Cary 5000). Photoluminescence (PL) emission spectra were recorded at room temperature with a luminescence spectrometer (Perkins Elmer LS55). Microstructural investigations were carried out by using FEI Tecnai-G^2 transmission electron microscope (TEM). Electron probe micro analyzer (EPMA) studies were carried out by using Cameca SX 100. Thicknesses of the deposited film were measured by using surface profilometer (Ambius Technology XP 200).

3. Results and discussions

Quantitative analysis for composition has been performed on $Zn_{0.6}Cd_{0.4}S$ films by EPMA. Across the center line of the laser target 50 points were taken for EPMA measurements. Uniform compositions were found across the target, suggesting compositional uniformity of the target. The molar ratios of Cd to Zn of the laser target obtained by EPMA were found as 0.407 ± 0.041. The obtained value of x was in agreement with the desired mole fraction in the laser target, and confirms the stoichiometry of the target. Thicknesses of all the deposited films were found in the range of 500–600 nm as measured by surface profilometer.

XRD patterns of the samples are shown in Fig. 1. Three diffraction peaks correspond to (100), (002) and (111) planes of the hexagonal crystalline $Zn_{0.6}Cd_{0.4}S$ with reflections positioned at $2\theta = 24.95^o$, 27.9^o and 32.18^o respectively. Semiconductor ternaries have been proposed to obey Vegard's law, revealing the linear relationship between the lattice constant and composition as follows [11]:

$$a^o_{A_{1-x}B_xC}(x) = (1-x)a^o_{AC} + xa^o_{BC}$$

where $a^o{}_{A_{1-x}B_xC}$ is the natural constant of the ternary form $A_{1-x}B_xC$ and a^o_{AC} and a^o_{BC} are the natural lattice constants of the binaries AC and BC respectively, and x is the mole fraction of binary BC{Hexagonal $a^o_{ZnS} = 3.777$ Å, $c^o_{ZnS} = 6.188$ Å (PDF 80-0007) and $a^o_{CdS} = 4.142$ Å, $c^o_{CdS} = 6.724$ Å (PDF# 01-0780)}. A close agreement between the experimental ($a = 3.92$ and $c = 6.408$ Å) and the theoretical lattice values ($a = 3.918$ and $c = 6.406$ Å) indicates that the composition of the ternary was very close to the mixing molar ratio of the starting materials of ZnS and CdS. As shown in Fig. 1, the diffraction peaks of the $Zn_{0.6}Cd_{0.4}S$ films formed at the laser incident flux density of 2.5 J/cm^2 are broad and weak. With increase in the laser incident energy from 2.5 J/cm^2 to, 3.33 J/cm^2 $Zn_{0.6}Cd_{0.4}S$ diffraction peaks become more intense and sharper. It is an indication of the improved crystalline quality of the samples. As the laser flux density is increased further to 4.16 J/cm^2, the intensity of diffraction peaks became weaker slightly, indicating that the crystalline quality of the samples degrades. In laser ablating and sputtering processes, a large amount of ions in the plasma are present. The emitted species appears to be highly peaked normal to the target surface. Kinetic energy of plasma species increases with increase in the laser flux density. When the plasma species reached upon the substrate surface, they congregated and grew as dense aggregates of independent nanoparticles with different sizes to form thin films. Improvement in the crystallinity of the films deposited at moderate laser flux density was due to sufficient atomic mobility that results in crystalline conformation [12]. However, too high laser incident flux density raises kinetic energy of ions and thus, may lead to too high plasma density. As the laser incident energy was increased to 4.16 J/cm^2, the direct bombardment of the ions led to induce a large structural disorder during film growth. Strain analysis has been carried out to find out the extent of strain that have induced in the thin films with laser flux density. Local strain is calculated by making use of Scherrer's formula of Δk vs k (the scattering vector $k = (4\pi/\lambda)Sin\,\theta$) [13]. In the inset of Fig. 1 local strain values are shown with variation in laser flux density. It can be seen from the inset that there is no observable change in the strain values when the laser flux density increases from 2.5 to 3.33 J/cm^2. However with further increase in laser flux density the local strain in the film increases due to the decrease in the crystallinity.

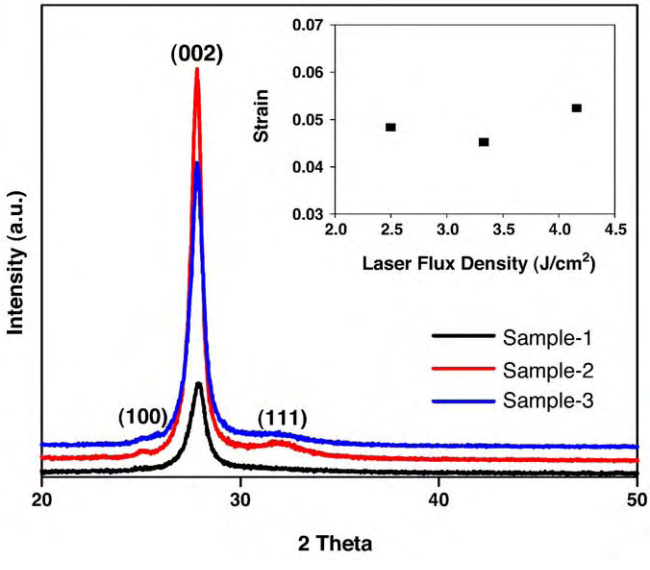

Fig. 1. X-ray patterns for the $Zn_{0.6}Cd_{0.4}S$ thin films formed at laser flux density of 2.5, 3.33 and, 4.16 J/cm^2. Inset: local strain values with laser flux density.

AFM images for samples deposited at the laser flux density of 2.5, 3.33 and 4.16 J/cm^2 are shown in Fig. 2. The AFM micrographs confirm that the films have a smooth surface with good adherence to the substrate and the spherical agglomerates have a narrow size distribution. With increase in laser flux density from 2.5 to 3.33 J/cm^2 there is an increase in particle size, and it is relatively uniform as shown in Fig. 2(b). Further increase in laser flux density to 4.16 J/cm^2 results in relatively large size particles as depicted in Fig. 2(c). The root-mean square roughness of the samples were measured over 2.0×2.0 μm^2 scanning range, and found 11.3, 4.8 and 20.1 nm for the samples with laser flux density of 2.5, 3.33 and, 4.16 J/cm^2 respectively. During the film growth, species (ions and neutrals) are propagating with various velocities reaching the surface of the film. The higher energy component of plume was related to ions, while neutral particles can obtain their velocities by collisions with fast ions. When the plasma formed under these conditions of the laser incident flux of 4.16 J/cm^2, led to the ions with too high kinetic energy. The atoms on the growing films could be bombarded and sputtered by incident ions with too high kinetic energy. While, a few large size neutral particles or debris could be emitted from the target under very high laser incident energy ablation, results in too coarsening and the large non uniformity of particle size. A destructive effect due to high energy could lead to deterioration of the growing films.

Please cite this article as: S. Singhal, et al., Thin Solid Films (2009), doi:10.1016/j.tsf.2009.09.115

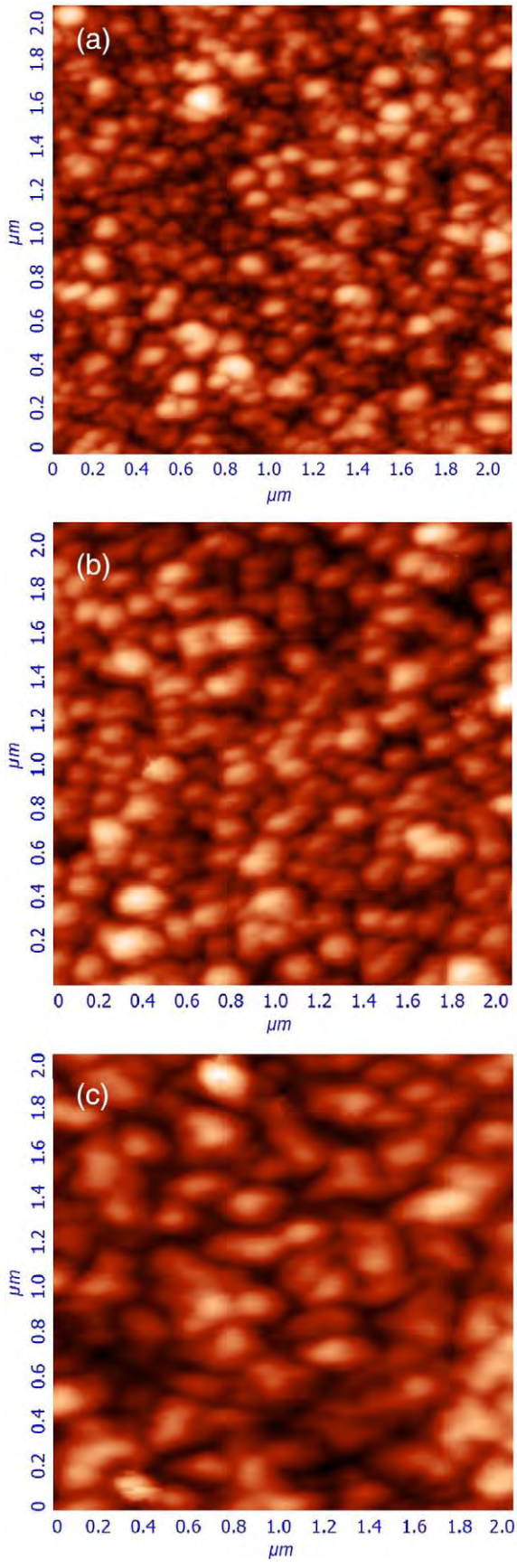

Fig. 2. Surface topography of the $Zn_{0.6}Cd_{0.4}S$ thin films formed at the laser flux density of (a) 2.5 J/cm^2, (b) 3.33 J/cm^2, and (c) 4.16 J/cm^2.

Fig. 3(a) shows the TEM image for $Zn_{0.6}Cd_{0.4}S$ sample deposited at 400 °C with laser flux density of 3.33 J/cm^2. All samples show TEM images with nearly spherical particles and having average diameter of 15 nm as shown in Fig. 3 (a). One representative phase contrast image of nanoparticles of the sample is shown in Fig. 3(b). Continuous lattice fringes throughout the whole particle reveal the crystalline nature of the nanoparticle without any observable defect. Contrast of image depends on the electron scattering; thus, for similar lattice parameters, ZnS is expected to exhibit lower contrast compared to CdS, since it has fewer electrons per unit cell [14]. We do not observe any stepwise change in the contrast across the diameter of the nanocrystal; this suggests a random distribution of cations, instead of any heterostructured nanocrystal embedded in the film or a phase separation within the single nanocrystal. Fig. 3(c) shows the selected area electron diffraction pattern characteristic of a hexagonal phase. The interplanar distance calculated from the image is 3.19 Å that matches closely with that obtained from XRD (3.204 Å).

Photoluminescence measurements were done at room temperature. Fig. 4 shows the PL spectrum normalized by their corresponding absorbance of samples deposited at different laser flux density at an excitation wavelength of 375 nm satisfying the basic excitation energy requirement exceeding the band gap energy [15]. PL spectrum exhibit two emission bands: a self activated band centered at around 424 nm, along with blue and green band centered at 480 and 533 nm respectively. The emission peak at 424 nm is near band emission (NBE) and can be attributed to excitonic transitions (Energy band gap for $Zn_{0.6}Cd_{0.4}S$ is 2.95 eV, as confirmed by Vegard's law). Blue and green emission is related with defect related luminescence [16]. It can also be seen that the PL maxima shift slightly towards lower energies with increasing laser flux density. There is a decrease of PL energy due to the formation of recombination centers below the bandgap as concluded from the broadening of spectrum of sample-3 with respect to spectrum of sample-2. The recombination centers are caused by the dependence of the particle composition of the ablated plume on the laser flux density. At flux density of approximately 3.33 J/cm^2 the number of fast particles (atoms and ions) decreases and that of slow particles (cluster and droplets) increases. As a result, at flux density of approximately 4.16 J/cm^2, the films are preferentially formed by clusters and droplets, which cause grain boundaries during the film deposition [17]. These grain boundaries give rise to the formation of radiative recombination centers within the bandgap, lowering the energy positions of the PL Peaks. At the same time with increasing laser flux density from 3.33 to 4.16 J/cm^2 PL peak intensity decreases that can be attributed to the increased surface roughness with increase in laser flux density.

A measure of the quality of the film deposited is the peak intensity ratio (R) between the principal bound exciton i.e. near band edge emission (NBE) and defect center luminescence [16]. Inset in Fig. 4 is a plot of R versus laser flux density. R value indicates that better incident energy is around 3.33 J/cm^2. Since the defect center emission band is generally related with complexed defects or impurities, the high R value in $Zn_{0.6}Cd_{0.4}S$ films indicates a low concentration of these crystalline defects. It should also be pointed out here that these PL measurements were done at room temperature which again indicates the good quality of our samples.

The transmittance spectra for the samples deposited with different laser flux density are shown in Fig. 5a. The oscillations in the spectrum with wavelength are due to interference effect. Transmission data shows a transmittance of more than 70 % in the visible region. Transmission data is used to obtain the refractive index of the samples by using a model proposed by Manifacier et. al. [18]. Thus, the obtained values of the refractive indices are given in Table 1. Optical absorption spectra of films were recorded as a function of photon energy ($h\nu$) in the wavelength range 200–800 nm. In order to determine the direct optical band gap, we used the Tauc relationship [19]. It is observed from Fig. 5 (b) that the energy band gap of the

Please cite this article as: S. Singhal, et al., Thin Solid Films (2009), doi:10.1016/j.tsf.2009.09.115

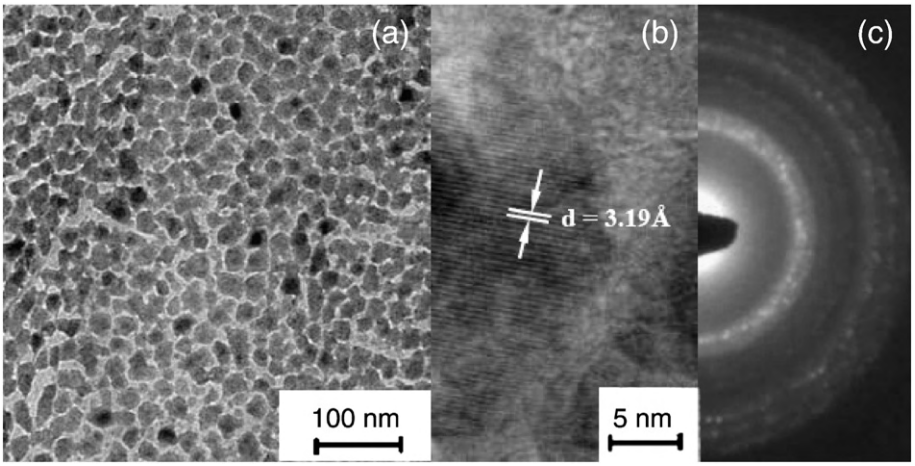

Fig. 3. (a) TEM image of $Zn_{0.6}Cd_{0.4}S$ sample deposited with laser flux density of 3.33 J/cm^2 (b) HRTEM image and ,(c) SAD pattern.

$Zn_{0.6}Cd_{0.4}S$ films decreases with increase in laser flux density. From XRD data we have found that there is a decrease in particle size with increase in laser flux density. Therefore the decrease in the energy band gap is attributed to increase in grain size.

4. Conclusions

The above results prove that the crystallinity, the surface quality and the optical properties of $Zn_{0.6}Cd_{0.4}S$ thin film are dependent on the laser flux density and the optimal incident energy is around 3.33 J/cm^2. The stoichiometric composition of the samples was in well agreement with the values obtained from Vegard's law. Surface morphology of the $Zn_{0.6}Cd_{0.4}S$ thin films is strongly dependent on the laser incident flux density and is confirmed via *R* value curve in addition to AFM micrographs. A slight decrease in PL peak energy is observed with increase in laser flux density. This decrease in band gap with increasing flux density is also validated by absorbance curves.

Acknowledgements

We are grateful to Dr. A. C. Pandey, Director, Nanophosphor Application Centre, Allahabad for providing the Photo Luminescence facility. The financial support by DST [Grant No.SR/S5/NM – 32/2005], New Delhi is gratefully acknowledged.

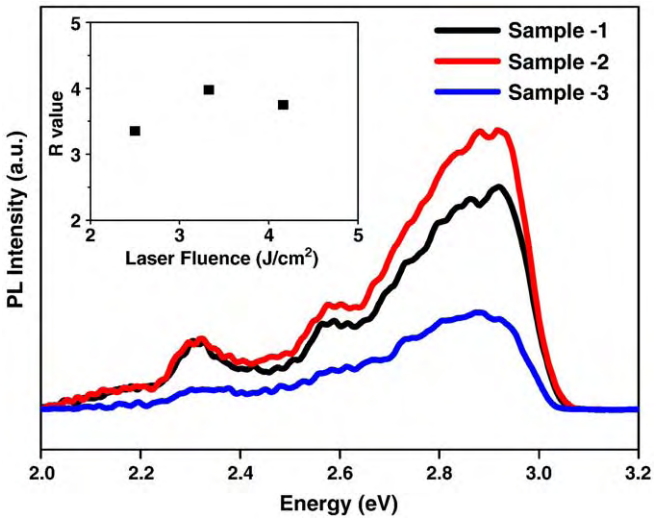

Fig. 4. PL properties of the UV-PLD films formed at a laser flux density of (a) 2.5, 3.33 and 4.16 J/cm^2; Inset is a graph between *R* value and laser flux density.

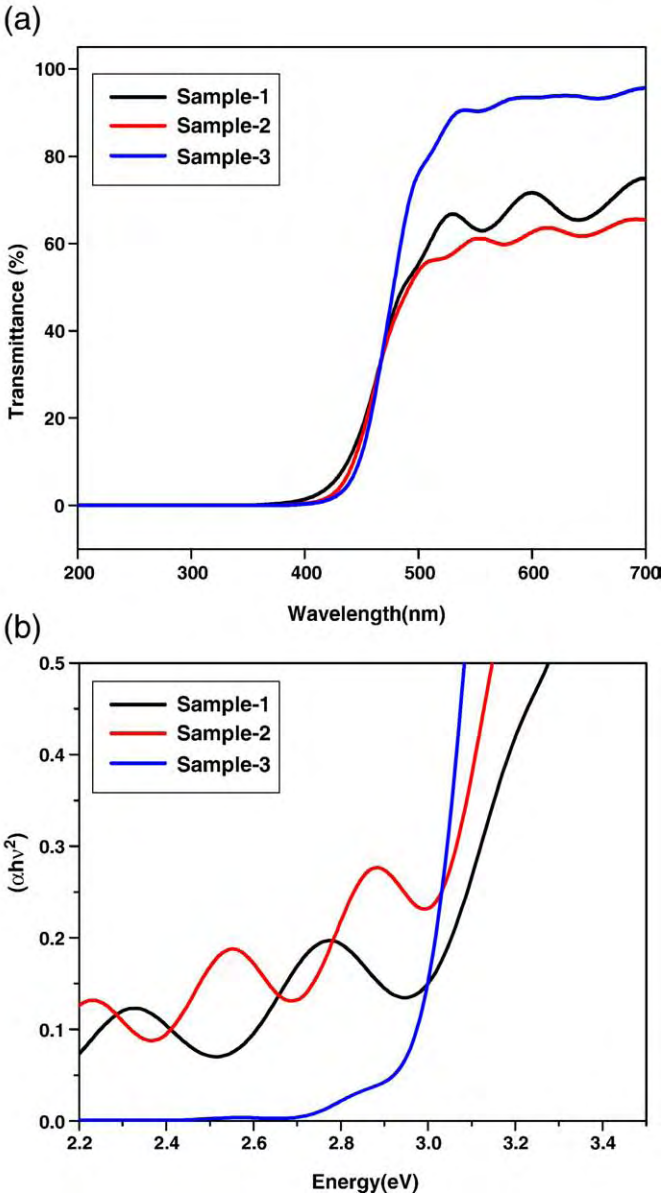

Fig. 5. (a) Spectral behaviour of optical transmittance $T(\lambda)$ (b) Profiles of $(\alpha h\nu)^2$ against $h\nu$ with varying laser flux density.

Please cite this article as: S. Singhal, et al., Thin Solid Films (2009), doi:10.1016/j.tsf.2009.09.115

References

[1] H.Y. Tang, C.C. Lin, L.S. Wang, K.H. Liao, F.Y. Liao, F.Y. Li, M.Y. Liao, Phys. Rev. B 77 (2008) 165420.
[2] A.P. Alivisatos, J. Phys. Chem. 100 (1996) 13226.
[3] D.J. Norris, Al.L. Efros, M. Rosen, M.G. Bawendi, Phys. Rev. B 53 (1996) 16347.
[4] M. Gunasekaran, M. Ichimura, Jap. J. Appl. Phys. 44 (2005) 7345.
[5] P.K. Schenck, M.D. Vaudin, D.W. Bonnell, J.W. Hasti, A.J. Paul, Appl. Surf. Sci. 655 (1998) 127.
[6] B. Ullrich, H. Sakai, Y. Segawa, Thin Solid Films 385 (2001) 220.
[7] H.S. Kwok, J.p. Zhang, S. Witanachchi, P. Mattocks, L. Shi, Q.Y. Ying, X.W. Wang, V.T. Shaw, Appl. Phys. Lett. 52 (1988) 1095.
[8] K.T. Hillie, C. Curren, H.C. Swart, Appl. Surf. Sci. 177 (2001) 73.
[9] A. Gupta, D.B. Chrisey, G.K. Hubler (Eds.), Pulsed Laser Deposition of Thin Films, Wiley, New York, 1994, p. 265.
[10] J.T. Chung, J. Madden, J. Vac. Sci. Technol. B 5 (1987) 705.
[11] J. Singh, Optoelectronics: An Introduction to Materials and Devices, Macgraw Hill, New Delhi, 1996.
[12] X.L. Tong, D.S. Jiang, Q.Y. Yan, W. Bhu, Z.M. Liu, M.Z. Luo, Vacuum 82 (2008) 1411.
[13] D. Son, D.R. Jung, J. Kim, T. Moon, C. Kim, B. Park, Appl. Phys. Lett. 90 (2007) 101910.
[14] X. Peng, M.C. Schlamp, A.V. Kadavanich, A.P. Alivisatos, J. Am. Chem. Soc. 119 (1997) 7019.
[15] T.H. Gfroerer (Ed.), Encyclopedia of Analytical Chemistry, John Wiley & Sons, 2000, p. 9209.
[16] T. Yao, M. Ogura, S. Matsuoka, T. Morishita, Appl. Phys. Lett. 43 (1993) 499.
[17] H. Zhao, E.P. Douglas, B.S. Harrison, K.S. Schanze, Langmuir 17 (2001) 8428.
[18] J.C. Manifacier, J. Gasiot, J.P. Fillard, J. Phys. E: Sci. Instrum. 9 (1976) 1002.
[19] A.K. Chawla, S. Singhal, H.O. Gupta, R. Chandra, Thin Solid Films 517 (2008) 1042.

Please cite this article as: S. Singhal, et al., Thin Solid Films (2009), doi:10.1016/j.tsf.2009.09.115